Journal of King Saud University – Computer and Information Sciences 31 (2019) 554–560

Contents lists available at ScienceDirect

Journal of King Saud University – Computer and Information Sciences

journal homepage: www.sciencedirect.com

Recognition of plastic surgery faces and the surgery types: An approach with entropy based scale invariant features

Archana Harsing Sable [a,*], Sanjay N. Talbar [b], Haricharan Amarsing Dhirbasi [c]

[a] School of Computational Sciences, Swami Ramanand Teerth Marathwada University, Nanded, Maharashtra, India
[b] Department of Electronics and Telecommunication Eng., Shri Guru Gobingji Singh Institute of Eng. & Tech., Nanded, M.S., India
[c] N.E.S. Science College, S.R.T.M. University, Nanded, India

ARTICLE INFO

Article history:
Received 2 November 2016
Revised 14 February 2017
Accepted 16 March 2017
Available online 18 April 2017

Keywords:
Face recognition
Plastic surgery
EV-SIFT feature
SVM classifiers

ABSTRACT

In recent years, the automatic recognition of face comprises many challenging problems which have experienced much consideration due to several applications in different fields. To solve all the situations like the pose, appearance, and lighting changes, and/or ageing the face recognition does not have many methods. The additional challenges which arise recently are Facial expression because of the plastic surgery. This paper deals with a new approach called Entropy-based Volume SIFT (EV-SIFT) for face recognition in an accurate manner after the plastic surgery. The analogous feature extracts the key points and volume of the scale-space structure for which the information rate is determined. Since the entropy is the higher order statistical feature this provides the least effect on uncertain variations in the face. For classification, the corresponding EV-SIFT features are applied to the Support vector machine. The normal SIFT feature extracts the key points on the basis of contrast of the image whereas the V- SIFT feature extracts the key points on the basis of the volume of the structure. Nevertheless, the EV-SIFT technique provides both the volume and contrast information. Finally, the experimental results demonstrate that the EV-SIFT are found to be better on recognizing the plastic surgery faces. Moreover, the methods are experimentally proven for recognizing the type of plastic surgeries such as Blepharoplasty achieves 98%, Brow lift achieves 97%, Liposhaving achieves 96%, Malar augmentation achieves 85%, Mentoplasty achieves 94%, Otoplasty achieves 99%, Rhinoplasty achieves 99% and Skin peeling achieves 91%.

1. Introduction

Generally, plastic surgery is used for improving the facial appearance (Sharma et al., 2014; Lee et al., 2012), for instance, removing scares, birthmarks and rectifying disfiguring defects (Zou and Yuen, 2012; Park et al., 2010; Mudunuri and Biswas, 2016). The attraction for plastic surgery is experienced worldwide and is determined by its characteristics like the affordable cost availability of advanced technology and the speed with which these procedures are performed (Sao and Yegnanarayana, 2007; Schwartz et al., 2012). However, the plastic surgery faces pose great challenges such as illumination variation in face components (Singh et al., 2009, 2010), occlusion (Liu et al., 2012), aging (De Marsico et al., 2016), security identifications and expression. Sometimes, the facial plastic surgery hides the identity of the genuine user and it might unintentionally refuse the genuine users. There are a lot of methods available to attain face recognition (Turk and Pentland, 1991; Ruiz-del-Solar and Navarrete, 2005; Lawrence et al., 1997; He et al., 2005; Inan and Halici, 2012; Lu et al., 2015). Plastic surgery face recognition (De Marsico et al., 2015; Kohli et al., 2015; Chude-Olisah et al., 2013; Bhatt et al., 2013) have undergone various developments in the recent past. The research contributions have been reported in the literature either in the feature extraction phase (De Marsico et al., 2015; Chude-Olisah et al., 2013; Bhatt et al., 2013) or in the classification phase (Kohli et al., 2015) or in both the phases. The classical feature descriptor, PCA (De Marsico et al., 2015) has the drawback of difficulties in determining the covariance matrix, though it exhibits reasonable computational time, handling high dimensional data and less sensitivity to noise. The prominent texture features such as local binary pattern (De Marsico et al., 2015) are computation-

* Corresponding author.
E-mail address: archanaharsingsable@gmail.com (A.H. Sable).
Peer review under responsibility of King Saud University.

Production and hosting by Elsevier

http://dx.doi.org/10.1016/j.jksuci.2017.03.004
1319-1578/

ally simple, but they lag in representing sensitive information. On the other hand, the projection matrix based classification reported as MPDL (Kohli et al., 2015) enable a simple classification process, yet they are not supportive of the natural environment. As per our review, very few contributions have been reported for classification, which is essential for recognition. Moreover, the feature descriptors have not been proposed sufficiently to discriminate inter-class faces. However, only few research contributions or methodologies have been reported in the literature to address the problem of recognizing the plastic surgery faces. Few of them include, the recognition using local region analysis (De Marsico et al., 2016), Shape Local Binary Texture Feature (SLBT) cascaded with periocular features (Lakshmiprabha and Majumder, 2012) and a combination of Gabor as well as LBP features (Lakshmiprabha et al., 2011). The Local region analysis (De Marsico et al., 2016) is very easy to calculate and have low intra-class variance and high extra-class variance. It means that the descriptor ought to be vigorous with respect to the aging of the subjects, alternating illumination etc. The SLBT (Lakshmiprabha and Majumder, 2012) computes the LBP feature histogram from shape free patch. Hence, the SLBT is very efficient to extracts the global shape variation through the local shape and shape modeling. The Gabor local binary pattern (GLBP) Lakshmiprabha et al., 2011 is used for localizing face shape landmark point in an image. This paper intends to recognize the faces even after the persons undergo plastic surgery followed by identifying the type of surgery. Hence, the contribution of the paper mainly considers three set of demonstrations. The first one is the detection of exact plastic surgery face using the novel SIFT feature based on entropy. The second one is to accurately recognize the true surgery portions while the third one is to analyze the performance of face recognition before and after plastic surgery. The organization of this paper as follows: In Section 2, relevant literature is briefly reviewed. Section 3 presents the Plastic surgery Face recognition. Experimental results are reported in Section 4. Finally, a conclusion is drawn in Section 5.

2. Related works

Chude-Olisah et al. (2013) have overcome the degradation in the performance of face recognition, which is caused due to the texture encoding process of the gray-level face image, through proposing a recognition scheme that involves an edge-based Gabor feature representation. The Gabor features are good descriptors and it provides an optimal resolution in both the time and frequency domains. However, the redundant illustration of the image by integrating the entire gathered image into superposition one to increase complexity.

De Marsico et al. (2015) have developed Principal Component Analysis (PCA) technique for accurate recognition of face which has undergone plastic surgery through the application of the region-based approaches. This PCA technique has features such as low noise sensitivity and low computation time. The PCA technique reduces the memory as well as capacity requirements and it provides the greater efficiency for processes involving smaller dimensions. However, the PCA technique fails to capture the simplest invariance and it is very difficult to evaluate the covariance matrix accurately.

Kohli et al. (2015) have described the projection matrix method to recognize normal faces, even after the modification of faces due to plastic surgery. This method subsists in linear algebra to acquire the best fit solution of a system of linear equations. This method requires less computational time and simple orthographic projection. Nevertheless, the image representation is not viable and it suffers from the convergence problems and the stability.

Bhatt et al. (2013) have introduced a multi-objective evolutionary granular algorithm, which supports in the matching of images that were taken prior and later to plastic surgery. The multi – objective evolutionary algorithm supports the problems requiring multiple solutions and the parallel implementation could be achieved with ease. On the other hand, the trial-and-error methodology of parameter tuning consumes more time and it is very expensive.

3. Plastic surgery face recognition

Fig. 1 demonstrates that the block diagram of the EV-SIFT based plastic surgery.

In the face recognition, there are two phases takes place like testing phase and training phase. For learning the EV-SIFT features of the pre-surgery is deal with the SVM in the training phase. To determine the actual subject the unknown plastic surgery faces are intended in the testing stage. Additionally, the SCM classifier recognizes the face accurately through the acquired learning information. In the proposed methodology as in Fig. 1, the image for testing is initially applied to the scale-space extrema detection block, where it determines the distinct points and its surrounding patches. Further, the DOG scale space is applied to extract the features of the face image. To the next of the feature extraction, the significant key points are extracted in the preceding block, and it eliminates both the extreme points and edge points. Meanwhile, the orientation and gradient module are determined for each extracted key point, from which the volume function and entropy function are estimated. Though the EV-SIFT contain both the volume and contrast of the image, the volume function and entropy function is combined to obtain a paired function. Subsequently, the resultant paired function is applied to the SVM classifier to perform optimum recognition.

3.1. Feature extraction using EV-SIFT

Let F_j be the face image and the I_i^D be the database with $i = 1, 2 \ldots N_D$ that have to satisfy the condition $F_j \subset I_i^D$ here $j = 1, 2 \ldots N_S$ and the size of the database I_i^D be $(M \times N)$.

The pre-processing stage starts with image resizing. The Eq. (1) represents the resize model of the image here the S_M and S_N indicates the scaled number of columns and rows.

$$I(x,y) = I_i(m_r, n_r) = \frac{1}{S_M * S_N} \sum_{u=(m_r-1)S_M}^{m_r S_M} \sum_{v=(n_r-1)S_N}^{n_r S_N} I_i(u,v) \tag{1}$$

In Eq. (1), $u \in [1, M]$ and $v \in [1, N]$, $0 \leqslant m_r \leqslant M_r - 1$ and $0 \leqslant n_r \leqslant N_r - 1$, $(M_r \times N_r)$ is the size of the resized image, the term $[\cdot]$ indicates the round-off function of the nearest integer.

$$S_M = \left[\frac{M}{M_r}\right] \tag{2}$$

$$S_N = \left[\frac{N}{N_r}\right] \tag{3}$$

3.2. Image scale-space extreme detection

The SIFT method have the capability to generate the unique informative features about the image. The Eq. (4) indicates the image scale-space representation of the two-dimensional image. Here, $G(x, y, \sigma)$ represents the variable-scale Gaussian function, σ represents the scaled coordinate and (x, y) is the spatial coordinate.

$$L(x, y, \sigma) = G(x, y, \sigma) I(x, y) \tag{4}$$

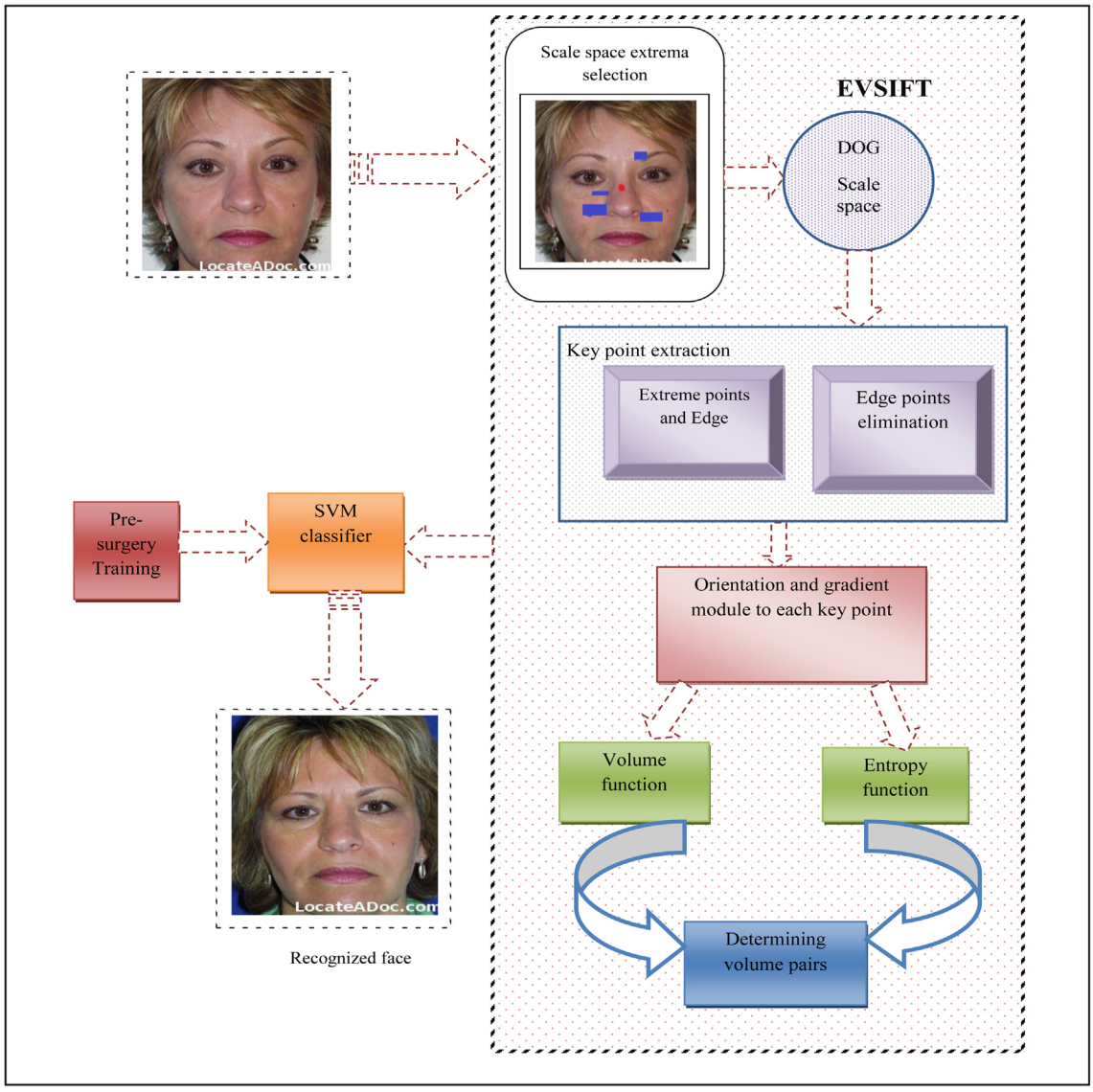

Fig. 1. Block diagram of EV-SIFT based plastic surgery face recognition.

3.3. Implement DOG scale space

In SIFT features the Difference of Gaussian (DOG) has many advantages. Since when the noise is added to the image or it is blurred in the geometric transformation the stability of the extracted feature points is not good. Hence for perfect matching, it is very necessary to extract the more stable feature points. The DOG aids to extract more scale-invariant features and the DOG scale space is established by means of the image scale space function and it is determined as follows,

$$D(x,y,\sigma) = L(x,y,k\sigma) - L(x,y,\sigma) \tag{5}$$

$$D(x,y,\sigma) = G(x,y,k\sigma) - G(x,y,k\sigma))I(x,y) \tag{6}$$

where $G(x,y,\sigma) = \frac{1}{2\sigma^2} e^{\frac{-(x^2+y^2)}{2\sigma^2}}$ represents the Gaussian function in the Eq. (6). In the DOG scale space, each sample point of the image is compared to 26 neighbours to identify the 2D image space and all the intense points. In the current image, the target point is needed to compare with 8 neighbours and also it compares with 18 neighbours in the scale below and above. In variance, the true scale can be estimated from the normalization of Laplacian, $\sigma^2\Delta^2 G$ with the factor σ^2. Subsequent to convolution by means of the normalized Laplacian function, the automatic scale selection can be accomplished as follows,

$$O(x,y,\sigma^2) = \sigma^2\Delta^2 GI(x,y) = \sigma^2\Delta^2 L(x,y,\sigma^2) \tag{7}$$

The Eq. (7) represents the output that is calculated from the convolution of the image with $O(x,y,\sigma^2)$. If the scale of the image structure is close to the σ value of the normalized Laplacian function the Eq. (7) will be at an extremum. In both the spatial space and scale space the points which are extrema should be chosen in terms of identifying the blob structure and choosing them at best scale.

3.4. Obtain the EV-SIFT key points

At the scale-space extrema the next point is to decide the key points in the difference of the Gaussian function and it is demonstrated with the image. Moreover, the key point parameters are completely relying on the distribution property of the gradient operation of the image that is on the key points. Hence, the key point gradient modules and orientation modules are computed

that registers invariance towards the image rotation. The orientation and gradient magnitude are computed for each sample and they are represented as

$$\theta(x,y) = \tan^{-1}\left(\frac{(L(x,y+1)-L(x,y-1))^2}{(L(x+1,y)-L(x-1,y))^2}\right) \quad (8)$$

$$m(x,y) = \left(\sqrt{\begin{array}{c}(L(x+1,y)-L(x-1,y))^2 \\ +(L(x,y+1)-L(x-1,y-1))^2\end{array}}\right) \quad (9)$$

The Eqs. (8) and (9) implies the $\theta(x,y)$ represents the orientation of the key point, $m(x,y)$ represents the gradient magnitude and the $L(x,y)$ represents the image sample. Besides, the scales that are utilized by the L are the corresponding scale for each key point. From the gradient operation of sample points within the region around the key point an orientation histogram is attained.

3.5. Entropy-based feature descriptor

In an image, the entropy is used to measure the unforeseeable of the content of the information. It describes the statistical measures of the randomness that can be used to describe the texture of an input image. The higher order statistical feature has the least effect because of the entropy on uncertain variations in the face.

The following steps illustrates the Entropy-based feature descriptor

Step 1: The V-SIFT formulation referred from Geng and Jiang (2009) is used to calculate the volume of the image and it is represented in the form of a matrix which is expressed in the Eq. (10)

$$V(i,j) = \begin{bmatrix} v(i_1,j_1) & v(i_1,j_2) & \cdot & v(i_1,j_n) \\ v(i_2,j_1) & v(i_2,j_2) & \cdot & v(i_2,j_n) \\ \cdot & \cdot & \cdot & \cdot \\ v(i_m,j_1) & v(i_m,j_2) & \cdot & v(i_m,j_n) \end{bmatrix} \quad (10)$$

Step 2: The information basis is memoryless and stationary. The Eq. (11) illustrates the volume of the structure in the EV-SIFT analysis that is the probability function.

$$V_p(i,j) = \frac{V(i,j)}{\sum_i \sum_j V(i,j)} \quad (11)$$

Step 3: The entropy is computed from the volume of the structure. For the EV-SIFT process, the entropy computation is expressed as follows,

$$E(V) = -V_p(i,j)\log V_p(i,j) \quad (12)$$

The Eq. (12) states that if $E(V)$ is high entropy, then the volume is from an unvarying direction. As well as, if $E(V)$ is low entropy, then the volume is varied distribution. Hence, F_i^D describes the whole data base which attained final EV-SIFT descriptor. In order to choose the level of Gaussian blur of the image, the orientation and gradient magnitude with the entropy descriptors and the volume of the image are sampled by means of the scale of key points at the corresponding key point location. An 8∗8 neighbour window is a sample that is centered on the key point and subsequently divides the neighbour into 4∗4 child window. Thus, the gradient orientation histogram along with the eight bins is computed by each child window. Around each key point, each descriptor contemplates the 4∗4 array of histograms and each histogram contemplates 8 bins. Consequently, 4∗4∗8 = 128 dimension is attained that is the feature vector.

3.6. SVM based recognition

In the SVM classifier, the acquired EV-SIFT feature descriptor of the plastic surgery faces is applied. In the training dataset to identify the decision surface which has a maximum distance to the points of different classes is the major concept of the SVM. In Eq. (13), the basic formula of the SVM classifier is represented as

$$S_v = w^T F_i^D + b \quad (13)$$

In Eq. (13), $w^T F_i^D + b = -1$ correspond to the negative support vectors and $w^T F_i^D + b = +1$ correspond to the positive support vectors. Here, b is the bias applied to the classifier and w is the weight vector. The main aim of this technique is to recognize the faces which have been subjected to the plastic surgery owing to high ambiguity in the faces before and after surgery.

4. Results and discussion

4.1. 1Experimental setup

The experiment of face recognition is conducted by different surgeries such as Blepharoplasty surgery for 68 faces, Browlift, Liposhaving surgery for 51 faces, Malar augmentation surgery for 51 faces, Mentoplasty surgery for15 faces, Otoplasty surgery for 18 faces, Rhinoplasty surgery for 52 faces, Rhytidectomy surgery for 72 faces, and Skin peeling surgery for 50 faces. Here, the surgery faces of 150 persons are present.

4.2. Statistical analysis

Table 2 summarizes the performance of EVSIFT features for plastic surgery. It is based on the different SVM kernel classifiers such as Linear, Quadratic, RBF and MLP. This Table demonstrates that the RBF gives better performance for different surgeries while comparing with other classifiers. In terms of the classifier RBF and Linear, the RBF performance is 21% for Blepharoplasty, 22% for Brow lift, 98% for Liposhaving, 17% for Malar augmentation, 28% for Mentoplasty, 26% for Otoplasty, 32% for Rhinoplasty, 26% for Rhytidectomy and 17% for Skin peeling better than the Linear classifier. In the case of classifier RBF and Quadratic, the performance of RBF is 21% better than the Quadratic classifier for Blepharoplasty, 12% better than the Quadratic classifier for Brow lift, 14% better than the Quadratic classifier for Liposhaving, 20% better than the Quadratic classifier Malar augmentation, 13% better than the Quadratic classifier for Mentoplasty, 14% better than the Quadratic classifier for Otoplasty, 12% better than the Quadratic classifier for Rhinoplasty, 17% better than the Quadratic classifier for Rhytidectomy, 16% better than the Quadratic classifier for Skin peeling. 57%, 86%, 19%, 10%, 98%, 15%, 25%, 13% and 76%.In terms of MLP and RBF classifiers, the RBF classifier performance is 57%, 86%, 19%, 10%, 98%, 15%, 25%, 13% and 76% for different surgeries such as Blepharoplasty, Browlift, Liposhaving, Malar augmentation, Mentoplasty, Otoplasty, Rhinoplasty, Rhytidectomy and Skin peeling. Hence, the performance of the RBF is better while comparing with all other classifiers.

4.3. K-fold cross validation

The original samples are randomly partitioned into k equal sized sub-samples in the k-fold cross validation. For testing the model, the single subsample is maintained as the corroboration data while the residual k-1 subsamples are used as training data. Here, the cross-validation is repeated k times (five folds), with each of the k subsamples used exactly once as the validation data. To

produce a single estimation the k results from the folds can then be averaged

The Table 1 clearly show that the RBF classifier performs better for the EV-SIFT feature for different plastic surgery while comparing with other classifiers such as Linear, Quadratic and MLP. Hence, Table 2 illustrates the experimental analysis of K-Fold cross-validation for RBF. This Table demonstrates that the different K-fold experiment like First fold, a second fold, third fold, fourth fold and Fifth fold for different plastic surgeries.

4.4. Impact of SIFT dimension

Two main parameters such as radius and Enlarge Factor (EF) are present in SVM classifier. These factors are varied and the performance analysis is performed. The impact of SIFT feature is shown in Table 3. The value for the radius is varied from 2.5, 5, 10, 15 and 20 where the corresponding value of EF is varied from 0.5, 1, 1.3, 1.5 and 1.7.

Table 3 demonstrates that the impact of EV-SIFT features based on its performance measures with radius = 0.5, 1, 1.3, 1.5 and 1.7 and EF = 0.5, 1, 1.3, 1.5 and 1.7. For radius = 5, the accuracy, sensitivity, specificity, precision, FPR, FNR, FDR, NPV, F1_score and MCC is better for EF = 1.7. At radius = 10, the performance measure is better for EF = 1.5 and 1.7. For radius = 15, the accuracy and sensitivity of EF = 1.5 is better, the specificity and precision of EF = 1.3, 1.5 and 1.7 is same and the FPR, FNR, FDR is better for 1.3, 1.5 and 1.7, the F1_score and MCC is better for EF = 1.5. For radius = 20, the accuracy and sensitivity is better at EF = 1.5 and the specificity and precision of EF = 1, 1.3 and 1.5 is same and the FPR remains same for all EF and the FNR, FDR is better for 1.5 and 0.5 and the F1_score and MCC is better for EF = 1. For radius = 25, the accuracy is better for EF = 1.3 and the sensitivity is better for 1.3and 1.5. From this inspection, it is clear that there is no fixed value for the radius and EF and the performance of SVM classifier gets better while varying these factors.

4.5. Performance measures of PCA, SIFT, V-SIFT and the proposed EV-SIFT method

Table 4 demonstrates that the comparison features of Principle Component Analysis (PCA) method; SIFT method, Volume SIFT method and the proposed method EV-SIFT. These features are analyzed based on the performance measures. Moreover, the analysis of the classifiers such as linear SVM, quadratic SVM, RBF SVM and MLP SVM for with plastic surgery is depicted in Fig. 2.

The performance of the algorithm is evaluated using renowned and widely applied error functions and their derivatives such as accuracy, sensitivity, specificity and much more (Powers, 2011; Altman and Bland, 1994). The accuracy is used to determine the degree of correctly classified face. Sensitivity is used to measure the method to correctly identify both the positive and negative samples. Here, the precision has the ability to give the ratio of positive against all the positive results. The FPR, FNR, NPV and FDR are used to correctly predict the correct identification and incorrect identification. The F1_Score and MCC are used to determine the correctness of the classification algorithm and the efficiency of binary class classification.

In Fig. 2(a), demonstrates the analysis of linear SVM. The performance measures are performed for the PCA, SIFT, V-SIFT and the proposed EV-SIFT based on the FPR, FNR, and FDR. The graph clearly shows that the FPR, FNR, and FDR of the proposed EV-SIFT are very low while comparing with the other feature method. Fig. 2(b) indicates that the Quadratic analysis of SVM. Here, the FPR, FNR, and FDR are very low for the EV-SIFT method. Hence, the performance of the EV-SIFT is better. Fig. 2(c) and (d) illustrates the analysis of RBF SVM and MLP SVM. Here, the performance measures such as FPR, FNR, and FDR for the PCA, SIFT, V-SIFT and the proposed EV-SIFT based is performed. Finally, the graphical representation clearly illustrates for the proposed EV-SIFT the FPR, FNR and FDR are very low while comparing with other methods such as PCA, SIFT, V-SIFT. Fig. 2(e), which is the linear SVM, the accuracy is better for the PCA while the sensitivity and the specificity are better for the EV-SIFT feature for plastic surgery faces. But here all the measures are better for the EV-SIFT feature. The performance is best for EV-SIFT feature when compared to the other feature extraction methods in linear SVM. Here, the accuracy of plastic surgery face recognition by the proposed EVSIFT feature is 10% better than PCA feature, 2% better than SIFT feature, and 1% better than VSIFTT feature. Fig. 2(f) demonstrates the performance measures of quadratic SVM. Here, the accuracy of the proposed EVSIFT feature for with plastic surgery is 1% better than the PCA feature, 4% better than the SIFT feature and 1% better than the VSIFT feature.

Table 1
Performance analysis on recognizing various plastic surgeries.

Classifiers	Performances of EVSIFT	Blepharoplasty	Brow lift	Liposhaving	Malar augmentation	Mentoplasty	Otoplasty	Rhinoplasty	Rhytidectomy	Skin peeling
Linear	Best	0.81	0.79	0.79	0.8	0.74	0.78	0.75	0.78	0.83
	Worst	0.75	0.77	0.74	0.70	0.70	0.73	0.72	0.70	0.75
	Mean	0.78	0.78	0.77	0.74	0.75	0.75	0.73	0.74	0.78
	Median	0.77	0.78	0.78	0.72	0.74	0.75	0.73	0.74	0.77
	Deviation	0.03	0.02	0.03	0.05	0.02	0.02	0.01	0.03	0.02
Quadratic	Best	0.86	0.87	0.86	0.79	0.84	0.86	0.88	0.84	0.84
	Worst	0.85	0.85	0.83	0.76	0.81	0.84	0.86	0.84	0.85
	Mean	0.86	0.87	0.84	0.78	0.82	0.85	0.87	0.84	0.86
	Median	0.85	0.87	0.84	0.77	0.81	0.85	0.87	0.84	0.85
	Deviation	0.004	0.01	0.01	0.01	0.02	0.007	0.008	0.001	0.004
RBF	Best	0.99	0.98	0.98	0.94	0.95	0.98	0.99	0.99	0.98
	Worst	0.99	0.98	0.98	0.94	0.95	0.98	0.99	0.99	0.99
	Mean	0.99	0.98	0.98	0.94	0.95	0.98	0.99	0.99	0.99
	Median	0.99	0.98	0.98	0.94	0.95	0.98	0.99	0.99	0.99
	Deviation	0.0001	0.02	0.0003	0.002	0	0	0.0001	0.0001	0.001
MLP	Best	0.98	0.97	0.96	0.85	0.94	0.97	0.99	0.99	0.91
	Worst	0.96	0.96	0.96	0.81	0.92	0.96	0.97	0.98	0.96
	Mean	0.97	0.97	0.96	0.84	0.94	0.96	0.98	0.98	0.98
	Median	0.97	0.97	0.96	0.85	0.94	0.97	0.98	0.98	0.97
	Deviation	0.007	0.09	0.003	0.02	0.02	0.003	0.007	0.005	0.07

Table 2
Results from K-fold cross-validation analysis.

Different surgeries	First fold	Second fold	Third fold	Fourth fold	Fifth fold
Blepharoplasty	0.933673	0.928571	0.933673	0.928571	0.916667
Brow lift	0.917355	0.917355	0.917355	0.917355	0.857143
Liposhaving	0.909091	0.909091	0.942149	0.92562	0.857143
Malar augmentation	0.666667	0.666667	0.666667	0.666667	0.777778
Mentoplasty	0.875	0.75	0.75	0.8125	0.5
Otoplasty	0.933884	0.909091	0.942149	0.917355	0.875
Rhinoplasty	0.946667	0.933333	0.937778	0.942222	0.933333
Skin peeling	0.937778	0.937778	0.937778	0.933333	0.930556

Table 3
The impact of EV-SIFT features based on its performance measures with radius and EF.

Rad	EF	Accuracy	Sensitivity	Specificity	Precision	FPR	FNR	FDR	NPV	F_1score	MCC
5	0.5	0.89	0.38	0.94	0.42	0.05	0.62	0.94	0.58	0.4	0.34
	1	0.87	0.35	0.93	0.4	0.07	0.65	0.93	0.6	0.37	0.30
	1.3	0.85	0.31	0.93	0.4	0.07	0.69	0.93	0.6	0.35	0.27
	1.5	0.88	0.42	0.95	0.55	0.05	0.58	0.95	0.44	0.48	0.42
	1.7	0.90	0.46	0.97	0.71	0.03	0.54	0.97	0.29	0.56	0.52
10	0.5	0.88	0.35	0.94	0.42	0.05	0.65	0.94	0.58	0.38	0.32
	1	0.90	0.42	0.964	0.59	0.03	0.58	0.96	0.41	0.49	0.43
	1.3	0.84	0.34	0.95	0.58	0.05	0.66	0.97	0.42	0.43	0.36
	1.5	0.91	0.5	0.98	0.76	0.02	0.5	0.975	0.23	0.60	0.57
	1.7	0.91	0.5	0.98	0.76	0.02	0.5	0.975	0.23	0.60	0.57
15	0.5	0.91	0.5	0.96	0.65	0.03	0.5	0.96	0.35	0.56	0.52
	1	0.92	0.52	0.98	0.81	0.01	0.48	0.98	0.18	0.63	0.61
	1.3	0.91	0.52	0.99	0.87	0.01	0.48	0.99	0.13	0.65	0.63
	1.5	0.93	0.56	0.99	0.87	0.01	0.44	0.99	0.13	0.68	0.67
	1.7	0.92	0.52	0.99	0.87	0.01	0.48	0.99	0.13	0.65	0.64
20	0.5	0.91	0.5	0.98	0.81	0.01	0.5	0.98	0.19	0.62	0.59
	1	0.93	0.54	0.99	0.88	0.01	0.46	0.99	0.13	0.67	0.65
	1.3	0.91	0.5	0.99	0.88	0.01	0.5	0.99	0.13	0.64	0.62
	1.5	0.92	0.51	0.99	0.88	0.01	0.48	0.99	0.13	0.65	0.63
	1.7	0.89	0.43	0.97	0.71	0.03	0.57	0.97	0.29	0.53	0.49
25	0.5	0.89	0.46	0.97	0.76	0.02	0.54	0.98	0.24	0.58	0.55
	1	0.90	0.46	0.98	0.76	0.02	0.54	0.98	0.24	0.58	0.56
	1.3	0.91	0.5	0.99	0.87	0.01	0.5	0.99	0.13	0.64	0.62
	1.5	0.90	0.5	0.97	0.76	0.03	0.5	0.97	0.24	0.60	0.57
	1.7	0.89	0.48	0.97	0.76	0.03	0.52	0.97	0.24	0.59	0.55

Table 4
Ranking of different SVM kernel using PCA, SIFT, V-SIFT and EV-SIFT with plastic surgery.

SVM classifiers	PCA	SIFT	VSIFT	EV-SIFT
Linear	3	2	4	1
Quadratic	2	3	4	1
RBF	4	2	3	1
MLP	1	2	3	4

Fig. 2(g), it describes the analysis for RBF SVM. Here all the measures are less for PCA, SIFT, and V-SIFT while the proposed EV-SIFT feature shows better performance. Moreover, the accuracy of plastic surgery face recognition by the proposed EVSIFT is 1% better than the PCA feature, 3% better than the SIFT feature and there is no variation between the VSIFT feature. In Fig. 2(h), all the measures show better performance while using the EV-SIFT feature. Here, the accuracy for with plastic surgery of the proposed EVSIFT feature is 1% better from PCA feature, 6% better from SIFT feature, 1% better from VSIFTT feature. Other feature extraction methods show poor performance. So by examining the overall analysis, it is clear that the EV-SIFT feature extraction is better for the plastic surgery face recognition purpose.

4.6. Sensitivity to plastic surgery faces

The ranking of the different kernel of SVM classifiers like linear, quadratic, RBF and MLP is shown in Table 3. This table depicts the rank of EV-SIFT is better whereas the rank of the other method is less. The Table 3 shows that the proposed EVSIFT features perform 67% better than the PCA, 27% better than the SIFT, 59% better than the V-SIFT for Linear. In terms of Quadratic, 67%, 27%, 58% better than the PCA, SIFT, and V-SIFT. In RBF, the proposed EVSIFT feature is 20% better than PCA, 12% better than SIFT, and 32% better than V-SIFT. In the case of MLP, the proposed EVSIFT feature performance is 59%, 27%, and 67% better than the existing features such as PCA, SIFT, and EVSIFT. Therefore, it is clear that the proposed EV-SIFT feature is highly sensitive to plastic surgery faces.

5. Conclusion

This paper deals with the face recognition method that uses the derived features on the basis of the EV-SIFT approach. The corresponding system was evaluated by using different surgeries such as Blepharoplasty, Browlift, Liposhaving, Malar augmentation, Mentoplasty, Otoplasty, Rhinoplasty, Rhytidectomy and Skin peeling. The unwanted key points are effectively removed by the proposed EV-SIFT method. Here, the proposed EV-SIFT approach

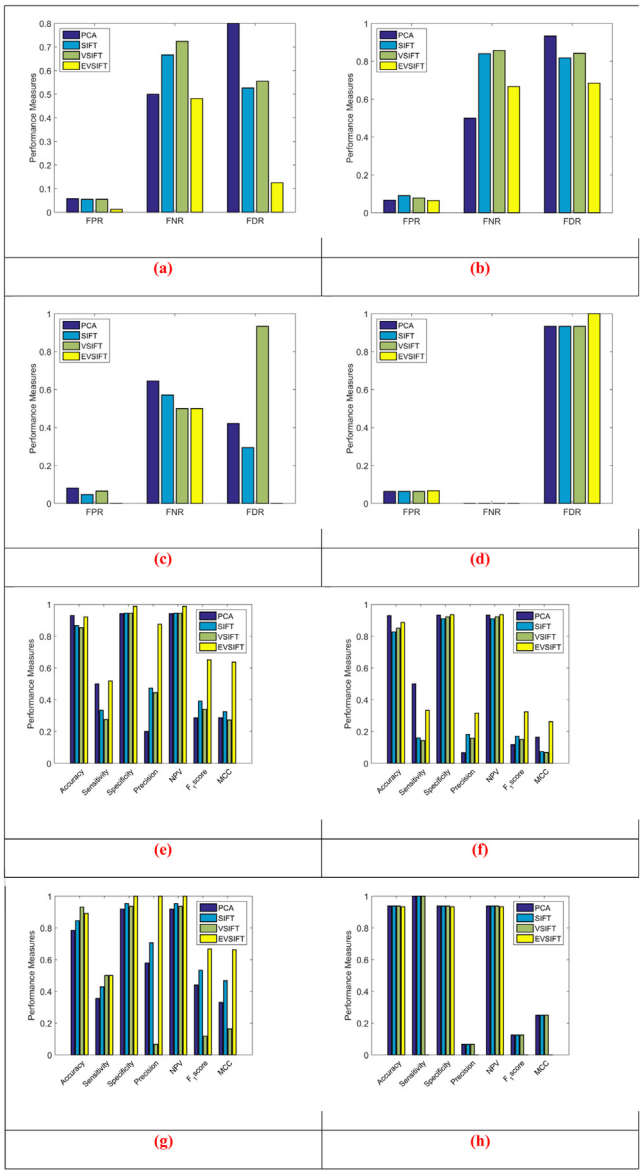

Fig. 2. Graphical representation of EV-SIFT features based on its perfomance measures (a) and (e) represents Linear SVM, (b) and (f) represents Quadratic SVM, (c) and (g) represents RBF SVM and (d) and (h) represents MLP SVM.

has obtained the volume of the structure and the contrast of the image. For the recognition purpose, the extracted features are applied to the SVM classifier. In the different kernel of SVM with the different existing features, the performance measures were analyzed. To produce the better performance, the EV-SIFT feature was very effective. The SVM classifier parameters like radius and enlarge factor was not fixed. It was clear from the analysis the performance was better for varied values of radius and EF and it was not fixed. Hence, the proper tuning was needed to obtain the fixed value. Future work will be aimed towards the analysis on the basis of the tuning process to obtain the accurate recognition of plastic surgery face.

References

Altman, D.G., Bland, J.M., 1994. Statistics notes: diagnostic tests 1: sensitivity and specificity. BMJ 308 (6943), 1552. PMC 2540489 Freely accessible. PMID 8019315.

Bhatt, Himanshu.S., Bharadwaj, Samarth, Singh, Richa, Vatsa, Mayank, 2013. Recognizing surgically altered face images using multiobjective evolutionary algorithm. IEEE Trans. Inf. Forensics Secur. 8 (1), 89–100.

Chude-Olisah, Chollette C., Sulong, Ghazali B., Chude-Okonkwo, Uche A.K., Hashim, Siti Z.M., 2013. Edge-based representation and recognition for surgically altered face images. In: Proceedings of the 2013 7th International Conference on Signal Processing and Communication Systems (ICSPCS), Carrara, VIC. pp. 1–7.

De Marsico, Maria, Nappi, Michele, Riccio, Daniel, Wechsler, Harry, 2015. Robust face recognition after plastic surgery using region-based approaches. Pattern Recogn. 48 (4), 1261–1276.

De Marsico, Maria, Nappi, Michele, Riccio, Daniel, Wechsler, Harry, 2016. Robust face recognition after plastic surgery using local region analysis. In: Image Analysis and Recognition, Lecture Notes in Computer Science, 6754. Springer, pp. 191–200.

Geng Cong, Jiang Xudong, 2009. Face recognition using SIFT features. In: 16th IEEE International Conference on Image Processing (ICIP). pp. 3313–3316.

He, Xiaofei, Yan, Shuicheng, Hu, Yuxiao, Niyogi, P., Zhang, Hong-Jiang, 2005. Face recognition using Laplacianfaces. IEEE Trans. Pattern Anal. Mach. Intell. 27 (3), 328–340.

Inan, Tolga, Halici, Ugur, 2012. 3-D face recognition with local shape descriptors. IEEE Trans. Inf. Forensics Secur. 7 (2), 577–587.

Kohli, Naman, Yadav, Daksha, Noore, Afzel, 2015. Multiple projective dictionary learning to detect plastic surgery for face verification. IEEE Access 3, 2572–2580.

Lakshmiprabha, N.S., Majumder, S., 2012. Face recognition system invariant to plastic surgery. In: 12th International Conference on Intelligent Systems Design and Applications (ISDA), Kochi. pp. 258–263.

Lakshmiprabha, N.S., Bhattacharya, J., Majumder, S., 2011. Face recognition using multimodal biometric features. In: Proceedings of the 2011 International Conference on Image Information Processing (ICIIP), Himachal Pradesh. pp. 1–6.

Lawrence, S., Giles, C.L., Tsoi, Ah Chung, Back, A.D., 1997. Face recognition: a convolutional neural-network approach. IEEE Trans. Neural Networks 8 (1), 98–113.

Lee, Sang-Heon, Kim, Dong-Ju, Cho, Jin-Ho, 2012. Illumination-robust face recognition system based on differential components. IEEE Trans. Consum. Electron. 58 (3), 963–970.

Liu, Xin, Shan, Shiguang, Chen, Xilin, 2012. Face recognition after plastic surgery: a comprehensive study. In: Computer Vision – ACCV 2012, Lecture Notes in Computer Science, 7725. Springer, pp. 565–576.

Lu, Ze, Jiang, Xudong, Kot, Alex C., 2015. A color channel fusion approach for face recognition. IEEE Signal Process. Lett. 22 (11), 1839–1843.

Mudunuri, Sivaram Prasad, Biswas, Soma, 2016. Low resolution face recognition across variations in pose and illumination. IEEE Trans. Pattern Anal. Mach. Intell. 38 (5), 1034–1040.

Park, Unsang, Tong, Yiying, Jain, Anil K., 2010. Age-invariant face recognition. IEEE Trans. Pattern Anal. Mach. Intell. 32 (5), 947–954.

Powers, David M.W., 2011. Evaluation: from precision, recall and F-measure to ROC, informedness, markedness & correlation. In: J. Mach. Learn. Technol. 2 (1), 37–63.

Ruiz-del-Solar, J., Navarrete, P., 2005. Eigenspace-based face recognition: a comparative study of different approaches. IEEE Trans. Syst. Man Cybern. Part C 35 (3), 315–325.

Sao, Anil Kumar, Yegnanarayana, B., 2007. Face verification using template matching. IEEE Trans. Inf. Forensics Secur. 2 (3), 636–641.

Schwartz, William Robson, Guo, Huimin, Choi, Jonghyun, Davis, Larry S., 2012. Face identification using large feature sets. In: IEEE Trans. Image Process. 21 (4), 2245–2255.

Sharma, Poonam, Yadav, Ram N., Arya, Karmveer V., 2014. Pose-invariant face recognition using curvelet neural network. IET Biometrics 3 (3), 128–138.

Singh Richa, Vatsa Mayank, Noore Afzel, 2009. Effect of plastic surgery on face recognition: a preliminary study. In: IEEE Computer Society Conference on Computer Vision and Pattern Recognition Workshops, Miami, FL. pp. 72–77.

Singh, Richa, Vatsa, Mayank, Bhatt, Himanshu S., Bharadwaj, Samarth, Noore, Afzel, Nooreyezdan, Shahin S., 2010. Plastic surgery: a new dimension to face recognition. IEEE Trans. Inf. Forensics Secur. 5 (3), 441–448.

Turk, M.A., Pentland, A.P., 1991. Face recognition using eigenfaces. In: Proceedings of the IEEE Computer Society Conference on Computer Vision and Pattern Recognition, Maui, HI. pp. 586–591.

Zou, Wilman W.W., Yuen, Pong C., 2012. Very low resolution face recognition problem. IEEE Trans. Image Process. 21 (1), 327–340.